

COMMONWEALTH OF AUSTRALIA



DEPARTMENT OF  
HEALTH AND  
FAMILY SERVICES

**The Ratios of Effective Dose to Entrance Skin Dose  
and to Air Kerma for some Medical Sources**

by

**Keith N Wise**

Part 2

Pages 14 - 25



**Australian  
Radiation  
Laboratory**

ARL/TR124

Lower Plenty Road, Yallambie, Victoria 3085

Telephone: (03) 9433 2211 Facsimile: (03) 9432 1835

Email: [info@arl.gov.au](mailto:info@arl.gov.au) Internet: [www.health.gov.au/hfs/arl](http://www.health.gov.au/hfs/arl)

## REFERENCES

- Birch, R; Marshall, M and Ardran, G. *Catalogue of spectral data for diagnostic X-rays*. The Hospital physicists Association Scientific report Series 30; 1979.
- Cristy, M and Eckerman, K F. *Specific absorbed fractions of energy at various ages from internal photon sources. 1. Methods*. Oak Ridge National Laboratory report ORNL/TM-8381/V1; 1987.
- International Commission on Radiological Protection. *Recommendations of the International Commission on Radiological Protection*. Oxford:Pergamon Press; ICRP Publication 26, Annals of the ICRP 1 (3); 1977.
- International Commission on Radiological Protection. *1990 Recommendations of the International Commission on Radiological Protection*. Oxford:Pergamon Press; ICRP Publication 60, Annals of the ICRP 21 (1-3); 1991.
- International Commission on Radiological Protection. *Basic anatomical and Physiological data for use in radiological protection: the skeleton*. Oxford:Press; ICRP Publication 70, Annals of the ICRP 25 (2); 1995.
- International Commission on Radiological Protection. *Conversion coefficients for use in radiological protection against external radiation*. Oxford:Pergamon Press; ICRP Publication 74, Annals of the ICRP 26 (3/4); 1996.
- International Commission on Radiological Protection Units and Measurements. *Radiation Dosimetry: X-rays generated at potentials of 5 to 150kV*. ICRU report 17; 1970.
- International Commission on Radiological Units and Measurements. *Photon, electron and neutron interaction data for body tissues*. ICRU report 46; 1992.
- International Commission on Radiological Units and Measurements. *Quantities and units in radiation protection dosimetry*. ICRU report 51; 1993.
- Jenkins, T M; Nelson, W R and Bindi, A. *Monte Carlo transport of electrons and photons*. Proceedings of the International School of Radiation Damage and Protection, 8th Course; 24 September - 3 October 1987, Erice, Sicily, Italy.
- Jones, D G. *A realistic anthropomorphic phantom for calculating organ doses arising from external photon irradiation*. Radiation Protection Dosimetry 72, 21-29; 1997.
- Kramer, R; Zankl, M; Williams, G and Drexler, G. *The calculation of dose from external photon exposures using reference human phantoms and Monte Carlo methods. Part I: The male (ADAM) and female (EVA) adult mathematical phantoms*. Gesellschaft für Strahlen-und Umweltforschung München (GSF)-Bericht S-885; 1982.

Morris, N. *Doses received by radiation workers in Australia (1991)*. Australian Radiation Laboratory report ARL/TR116; 1994.

National Health and Medical Research Council. *Recommendations for limiting exposure to ionizing radiation (1995)*. Australian Government Publishing Service, Radiation Health Series No 39; 1995.

Nelson, W R; Hirayama, H and Rogers, D W O. *The EGS4 code system*. Stanford Linear Accelerator Center report SLAC-265; 1985.

Nowotny, R and Höfer, A. *Ein programm für die berchnung von diagnostischen Röntgenspektren*. Fortschr. Rontgenstr. 142, 6, 685-689; 1985.

Sakamoto, Y. *PHOTX data as PEGS4 cross-section data*. KEK proceedings 93-15; 1993.

Wall, B F and Jones, D G. *Organ doses from medical X-ray examinations calculated using Monte Carlo techniques*. National Radiological Protection Board Report R-186; 1985.

Wall, B F; Harrison, R M and Spiers, F W. *Patient dosimetry techniques in diagnostic radiology*. The Institute of Physical Sciences in Medicine Report 53; 1988.

Weber, D A; Eckerman, K F; Dillman, L T and Ryman, J C. *MIRD: radionuclide data and decay schemes*. New York: The Society of Nuclear Medicine; 1989.

Wise, K N. *An EGS4 based mathematical phantom for radiation protection calculations using standard man*. Health Physics 67:548-543; 1994.

Yamaguchi, Y. *Age-dependent effective doses for external photons*. Radiation Protection Dosimetry 55:123-129; 1994.

Zankl, M; Petoussi, N and Drexler, G. *Effective dose and effective dose equivalent - the impact of the new ICRP definition for external photon irradiation*. Health Physics 62:395-399; 1992.

Zankl, M; Drexler, G; Petoussi-Henß, N and Saito, K. *The calculations of dose from external photon exposures using reference human phantoms and Monte Carlo methods. Part VII: organ doses due to parallel and environmental exposure geometries*. Gesellschaft für Strahlen- und Umweltforschung München (GSF) report GSF-Bericht 8/97; 1997.

## APPENDIX A

### Monte Carlo methods with a mathematical phantom

The following sections give further detail on the Monte Carlo methods used in the calculations for Section 3.2.

#### A.1 Program outline

The computer simulation of radiation transport in idealised human subjects requires a model of the organs, their sizes, their relative positions and their chemical compositions. A simulation follows each particle incident on the body and their transport from the source to the body and then from organ to organ until the particle is absorbed or leaves the body. Mathematical descriptions of the organs have been provided for male and for female adults by Kramer et al (1982) and for models combining male and female characteristics by Cristy and Eckerman (1987). The present calculations use a computer model developed at ARL (Wise 1994) which incorporates all these mathematical phantoms. The program is based on the EGS4 code (Nelson et al 1985) which has been thoroughly tested and benchmarked against experimental data (Jenkins et al 1987). The transport algorithm used by EGS4 requires that the probability of competing transport processes be known. The data to generate the probabilities for each process are calculated by an additional program (PEGS4) using the compositions of the media through which the particles are transported. Details on the compositions of all media used in this study are given in Appendix A.2.

The mathematical phantom is interfaced to the EGS4 package via two mandatory subroutines known as HOWFAR and AUSGAB. The former routine, as its name implies, evaluates the distance to the next boundary along the particle trajectory while the latter routine enables the calculation of any physical quantity of interest including the energy deposited in each organ during particle transport. For the ARL implementation of the mathematical phantoms, HOWFAR has been structured to call other routines which calculate the distance to the boundary for particles exterior or interior to each organ. Other subroutines can be added by the user to perform additional calculations; for example, to sample the radiation emitted by the source, to derive the average energy deposited or to estimate the dose to an organ. The computer program is sufficiently flexible for the user to incorporate new regions into HOWFAR, to calculate additional quantities in AUSGAB or to perform specific calculations.

In the current version of the ARL phantom the following calculations are carried out by AUSGAB. Firstly, a cumulative sum of the energy deposited in each organ during particle transport is maintained. Secondly, factors for calculating the dose to bone marrow and to the bone surface are stored. Details on the methods used for calculating the dose to bone marrow and the bone surface are given in Appendix A.3. Finally, the phantom is covered by skin which is 2mm thick so that the skin entrance dose, denoted by  $H_p(1)$  in this report, is computed as the dose to user-specified regions on the skin surface by two methods:

- (a) directly from the energy deposited in these regions by transported particles and the mass of the tissue sample and

- (b) from the track-length,  $t_i$ , of photons crossing these regions, the photon energy,  $E_i$ , and the mass-energy absorption coefficient for tissue,  $(\mu_{en}(E)/\rho)$  as:

$$H_p(l) = \sum_i E_i t_i \left( \frac{\mu_{en}(E_i)}{\rho} \right) / V$$

where  $V$  is the volume of skin sample which is 2mm thick for adult phantoms (Cristy and Eckerman 1987).

The estimate from method (b) is expected to have a smaller uncertainty as all photons crossing the regions of interest are taken into account while for method (a) only those events producing an interaction contribute to the energy deposited. The mass-energy absorption coefficients in (b) are those tabulated for average tissue in ICRU report 46 (1992). For both methods the separate contributions of the primary photons and the photons scattered from the body to the entrance dose are also calculated to derive the back-scatter factor,  $BSF$ , which is defined as the ratio of the total dose to the tissue element to the dose contributed by primary photons only.

For all calculations the radiation field at the mid-plane spans the whole phantom. Electrons are not transported in the simulations; when electrons do appear their energy is deposited immediately (kerma approximation). The mathematical phantoms used in this work are the male and female phantoms referred to as ADAM and EVA (Kramer et al 1982).

## A.2 Media composition

Table A2.1 gives the compositions of the media adopted for input to PEGS4 to generate the data used by EGS4 to calculate the probabilities of the various physical processes. Four media are used in simulations discussed in this report - air, average soft tissue, lung and bone. For air, average soft tissue and lung, the compositions are based on those tabulated by the ICRU (1992). The soft tissue composition is the average of the ICRU values for adult men and women. The composition of bone given in this table is that used by Wall and Jones (1985) as the ICRU tabulations do not give average compositions for the whole skeleton.

**TABLE A2.1**

**Elemental composition of the media**

Element	Percentage of element in media			
	Air	Tissue	Lung	Bone
H		10.55	10.3	7.04
C		28.55	10.5	22.79
N	75.5	2.55	3.1	3.87
O	23.2	57.45	74.9	48.56
Na		0.1	0.2	0.32
P		0.2	0.2	6.94
S		0.25	0.3	0.17
Cl		0.15	0.3	0.14
Ar	1.3			
K		0.2	0.2	0.15
Mg				0.11
Ca				9.91
Density g.cm <sup>-3</sup>	0.0012	1.025	0.26	1.486
Reference	ICRU 1970	ICRU 1992	ICRU 1992	NRPB 1985

**A.3 Calculation of dose to bone marrow and to bone surface**

The calculation of the dose to the bone marrow and bone surface used in this report is based on Wall et al (1988). The method requires the estimation of two factors which are used to modify the estimate of dose to skeletal bone to produce the required doses. One factor is the ratio of the mass energy absorption coefficient for skeletal bone to those for bone marrow or endosteal tissue. The second factor is associated with the photoelectric enhancement of the dose to bone marrow or endosteal tissues. In practice, the dose to bone marrow or to the bone surfaces is calculated from an energy-weighted product of the photoelectric enhancement factor and the ratios of the mass energy absorption coefficients. Both of the factors are energy dependent. The final results for the dose to bone marrow are additionally weighted by the fraction of active marrow in the different bones as given by Cristy and Eckerman (1987). It is

assumed here that the ratio of mass energy absorption coefficients is independent of age while the photoelectric enhancement factor is age dependent as shown in the report of Wall et al (1988).

The dose to bone marrow is given by:

$$D_{RM} = D_{bone} [1 + g_{RM}(E, age)] (\mu_{en}/\rho)_{bone}^{RM}$$

where *age* is the mean age for the phantom model used in the calculation chosen from 0, 1, 5, 10, 15 and  $\geq 21$ y.

The dose to bone surfaces is given by:

$$D_{BS} = D_{bone} [1 + g_{BS}(E, age)] (\mu_{en}/\rho)_{bone}^{BS}$$

where  $g_{RM}$  is the fractional dose enhancement factor for bone marrow  
 $g_{BS}$  is the fractional dose enhancement factor for bone surface tissue  
 $\mu_{en}/\rho$  is the mass energy absorption coefficient. The ratios of the mass energy absorption coefficients have been based on the data of ICRU 46 (1992). Some values for the ratios are given in Table A3.1.

The enhancement factors also vary with the type of bone. However average values of  $g_{RM}$  for the whole skeleton are given in Table 5.1 of Wall et al as a function of age. Further, the mean path,  $L$ , across the marrow space also depends on age so that:

$$g_{RM}(E, age) = f_{RM}(E) / [100L_{RM}(age)]$$

where  $f_{RM}$  is an energy dependent factor which is identical to the percentage excess dose for cavity diameters of 1 millimetre. The values of  $f_{RM}$  may be found from Fig. 5.6 of Wall et al and are also given in Table A3.1.  
 $L_{RM}$  is the mean path across the marrow space in millimetres.

Regression of data for  $L_{RM}$  on the trunk length,  $C_T$ , for phantoms of different assigned ages gives the approximation:

$$L_{RM} = 0.329 + 0.0071C_T$$

where  $C_T$  is the length of the trunk in centimetres for a phantom representing individuals of  $age$  years.

The expression adopted to calculate the fractional enhancement is thus:

$$g_{RM}(E, age) = f_{RM}(E)/(32.9 + 7.1C_T)$$

For consistency, a similar approximation has been adopted to calculate the fractional dose enhancement factor for bone surfaces,  $g_{BS}$ , as:

$$g_{BS}(E, age) = f_{BS}(E)/(7.1 + 0.254C_T)$$

where  $f_{BS}$ , the percentage excess dose for a 1mm mean diameter of the trabecular spaces, is given in Table A3.1. The approximation is intended to fit the data of Table 5.2 of Wall et al. (1988) and is based on estimates of the diameter of trabecular spaces (ICRP 1995).

TABLE A3.1

Values of parameters as function of photon energy

Photon energy MeV	$f_{RM}$	$f_{BS}$	$(\mu_{en}/\rho)_{bone}^{RM}$	$(\mu_{en}/\rho)_{bone}^{BS}$
<0.010	0.00	0.00	---	---
0.01	1.5	5	0.20	0.56
0.02	2.2	7	0.17	0.553
0.03	3.3	10	0.167	0.553
0.04	8.0	21	0.182	0.562
0.05	10.5	28	0.219	0.581
0.06	8.6	22	0.28	0.616
0.08	6.4	11.5	0.454	0.710
0.10	4.4	6.4	0.634	0.807
0.12	2.6	3	0.741	0.865
0.14	1.06	1.1	0.848	0.922
$\geq 0.20$	0.00	0.00	1.0	1.0

Notes(1) mass energy absorption coefficients for bone, red marrow and bone surface are those for rib, red marrow and bone spongiosa given in ICRU 46, pages 101, 103 and 106, respectively.

## A.4 Validation

Validation of the program has been by comparison of the results obtained with it against the results published by others. Of relevance to this report are the results given by Yamaguchi (1994) and the ICRP (1996) for the ratio of the effective dose to air kerma  $E/K_{air}$  for exposure to monoenergetic parallel beams of radiation entering the body by a number of geometries including the AP, PA and ROT geometries defined in Section 1 as well as 2 lateral geometries in which the beam enters the body from the right side (RLAT) or from the left side (LLAT). The advantages of these comparisons are that the spectra of the incident radiations are unambiguous and the geometries are easily simulated.

### A.4.1 Effective dose to air kerma

Figure A4.1 compares the estimates of  $E/K_{air}$  for the AP, PA and RLAT geometries; the results for the ROT geometry overlaps those for the RLAT geometry and are not shown for clarity. Overall, the results of Yamaguchi (1994) and ICRP (1996) are in good agreement with those obtained with the EGS4 based code. However, a detailed comparison shows systematic differences at low energies. A similar comparison between the results of Yamaguchi and of the ICRP are discussed in ICRP (1996). Because Yamaguchi had used the androgenous phantoms of Cristy and Eckerman (1987), it was felt that the differences reflected the effects of the different phantoms. The ADAM and EVA phantoms used in this work are identical to those applied by the ICRP and therefore the differences are unlikely to be due to the phantom geometry. One explanation is that there are differences in the transport methodologies. The EGS4 code as applied to the present calculation selects the physical processes randomly according to the probability of each process occurring. The code on which the ICRP results are based (Zankl et al 1997) assumes for each interaction, that a photoelectric event occurs with known probability and that a photon continues, after a Compton scatter event, with the remainder of the probability. An alternative explanation for the differences is the possibility that the cross-sections are different. The calculations were repeated using the tissue compositions on which the ICRP results are based (Kramer et al 1992). To make the simulation as close as possible to that of Zankl et al, the transport processes were limited to the photoelectric and Compton scatter processes with photoelectric and bound Compton cross-sections being based on a PEGS4 implementation of the PHOTX libraries (Sakamoto 1993). While these modifications eliminated some of the differences between those calculated with the EGS4 based phantom and those reported by the ICRP in the 30-60 keV region, the differences were not completely removed. Figure A4.2 summarises the differences between the various results and those of the ICRP. The reason for the differences remain unexplained but may have their origin in the differing cross-sections used by the three groups.

For consistency with the results of the ICRP, the ratios reported in Section 3.1 are based on those of the ICRP and the analytical methods discussed in Section 2.3.1.

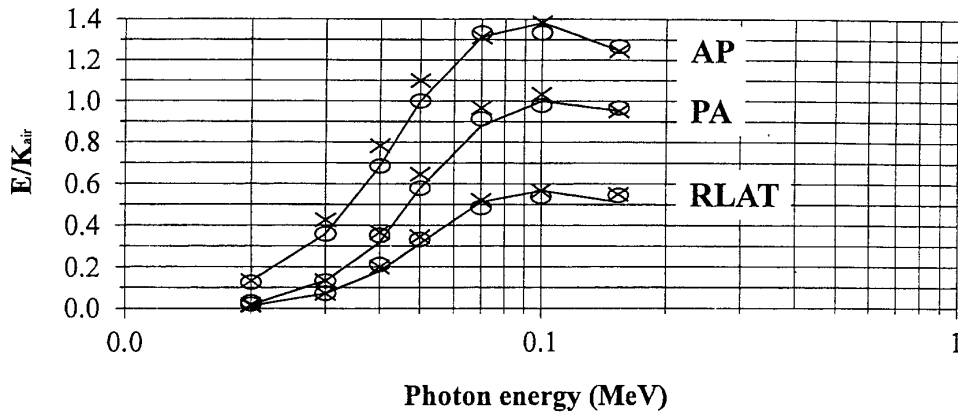


Figure A4.1 The ratio of effective dose to air kerma for monoenergetic parallel beams incident on a phantom as computed by ARL (—), ICRP 1996 (X), and Yamaguchi 1994

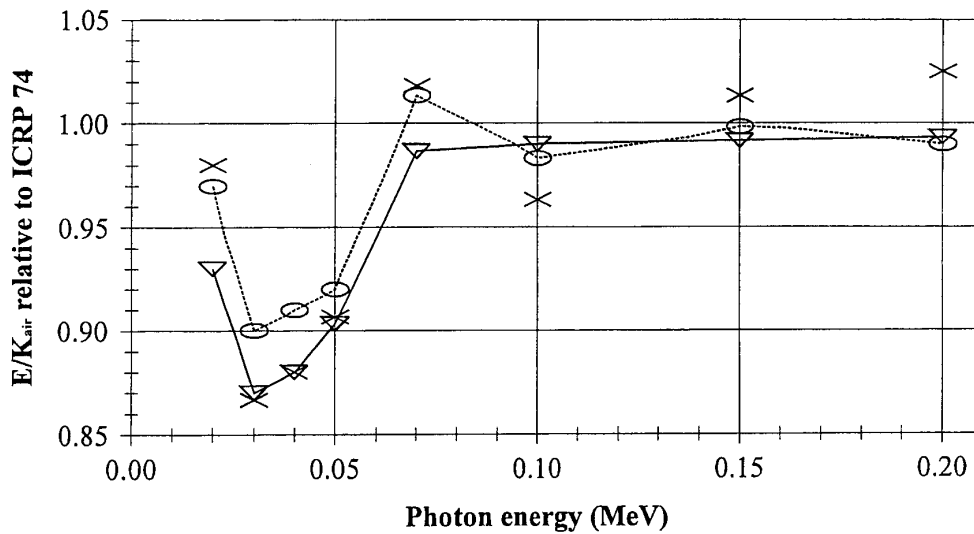


Figure A4.2 Ratio of effective dose to air kerma for a parallel monoenergetic beam incident on the front of a mathematical phantom as computed by Yamaguchi (1994) (X), ARL using ICRU tissue compositions (∇) and ARL using GSF compositions with PHOTX photoelectric absorption coefficients (○).

#### A.4.2 Effective dose to entrance skin dose

ICRP publication 74 table the personal dose equivalent for an ICRU slab at depths of 0.07mm and 10mm normalised to air kerma i.e.  $H_p(0.07)/K_{air}$  and  $H_p(10)/K_{air}$  respectively. The former ratio can be used as an estimate of the entrance skin dose normalised to air kerma so that  $E/ESD$  can be estimated, for monoenergetic radiation, from the ICRP tables by a simple division and for the spectra of Section 2.1 by application of equation (2.3.4). This approach is valid only for radiations incident on the body via AP geometry. For the PA and ROT geometries, where normalisation is to the skin dose to a region on the front of the body, Monte Carlo methods are required to estimate  $E/ESD$ .

The ADAM and EVA phantoms are covered by skin of 2mm thick; the skin on the phantom needs to be sufficiently thick so that adequate statistics on quantities related to this region can be calculated during Monte Carlo simulations. The absorbed dose to small regions on the skin surface are thus average values at a depth of 1mm; thus the entrance skin dose is denoted by  $H_p(1)$  in this report.

Fig. A4.3 shows the percentage difference of  $E/H_p(1)$  for the AP and PA geometries as calculated from the ADAM and EVA mathematical phantoms from  $E/H_p(0.07)$ . For the AP geometry the skin dose is evaluated at the anterior surface and for the PA geometry at the posterior surface of the phantom. The figure appears to show that the estimates of  $E/H_p(1)$  could be low by about 5%. However,  $H_p(0.07)/K_{air}$  is for an ICRU slab and neglects scatter from the bone and lung structures within the phantom.

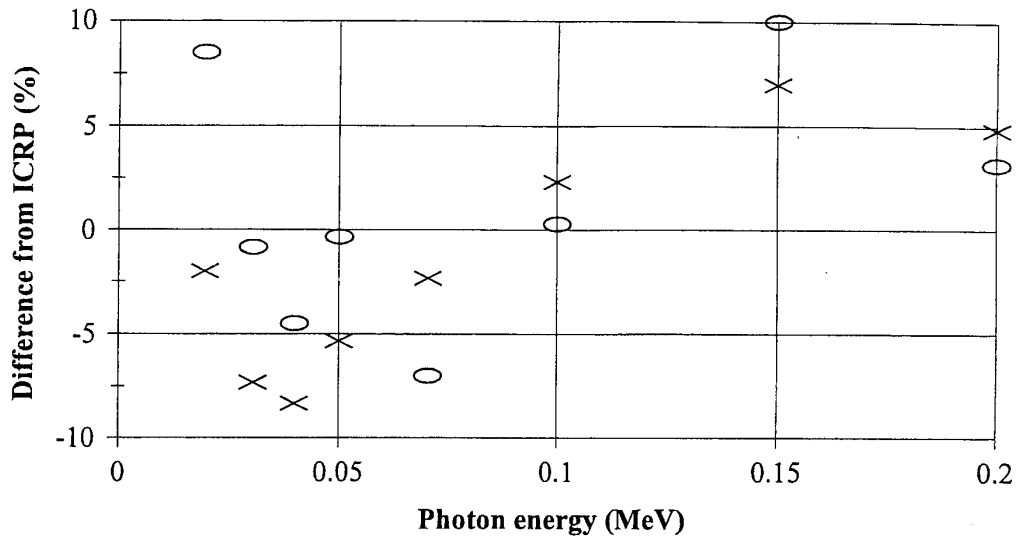


Figure A4.3 Differences of the ratio of effective dose to entrance skin dose, computed by the Monte Carlo method, from the ratio computed from ICRP (1996) for monoenergetic parallel radiation incident in AP geometry ( $\times$ ) and in PA geometry ( $\circ$ ). The entrance skin doses correspond to the dose to a small region of skin at the front and at the back of the phantom, respectively. As explained in the text, the ICRP values are derived from  $H_p(0.07)/K_{air}$  for the ICRU slab.